



## Design and Testing of a Graphite Foam-Based Supercooler for High-Heat-Flux Cooling in Optoelectronic Packages

Walter W. Yuen , Jianping Tu , Wai-Cheong Tam & Daniel J. Blumenthal

To cite this article: Walter W. Yuen , Jianping Tu , Wai-Cheong Tam & Daniel J. Blumenthal (2014) Design and Testing of a Graphite Foam-Based Supercooler for High-Heat-Flux Cooling in Optoelectronic Packages, Heat Transfer Engineering, 35:10, 913-923, DOI: [10.1080/01457632.2014.859513](https://doi.org/10.1080/01457632.2014.859513)

To link to this article: <http://dx.doi.org/10.1080/01457632.2014.859513>



Accepted author version posted online: 14 Nov 2013.  
Published online: 14 Nov 2013.



Submit your article to this journal [↗](#)



Article views: 89



View related articles [↗](#)



View Crossmark data [↗](#)

# Design and Testing of a Graphite Foam-Based Supercooler for High-Heat-Flux Cooling in Optoelectronic Packages

WALTER W. YUEN,<sup>1</sup> JIANPING TU,<sup>1</sup> WAI-CHEONG TAM,<sup>1</sup>  
and DANIEL J. BLUMENTHAL<sup>2</sup>

<sup>1</sup>Department of Mechanical Engineering, Hong Kong Polytechnic University, Hong Kong

<sup>2</sup>Department of Electrical and Computer Engineering, University of California at Santa Barbara, Santa Barbara, California, USA

*The feasibility of using graphite foam as a heat sink and heat spreader in optoelectronic packages is assessed. A “supercooler” is designed, fabricated, and tested to verify its cooling capability under high heat flux conditions in a typical optoelectronic package. The supercooler uses graphite foam as a primary heat transfer material. Water is soaked into the graphite foam, and under evacuated pressure, boiling is initiated under the heating region to provide enhanced cooling. Experiments were conducted for a heat flux of up to 400 W/cm<sup>2</sup> deposited over a heating area of 0.5 mm × 5 mm. Two-dimensional transient temperature distributions were recorded using a high-speed infrared camera. Data were obtained for steady heating, and for periodic heating with frequency up to 8 Hz. Results show that the supercooler is very efficient in dissipating heat away from the heating region. The average cooling rate during the cooling period exceeds 170 K/s.*

## INTRODUCTION

With the increased interest and advances in the design of optoelectronic devices [1] and the increase in the power level of lasers utilized in many future space-based communication applications, there is an increasing need for the development of an effective thermal management strategy to maintain temperature uniformity over surfaces at which miniature optical devices (with length scale of millimeters or less) are mounted in order to preserve optical alignment. The strategy must account for not only the dissipation of the high-density power generation (up to 400 W/cm<sup>2</sup>), but also the prevention of large temperature gradient on the device surface during rapid transient heating, with typical time scales as short as a few microseconds. Effective thermal spreading and heat dissipation are important challenges that must be met by modern optoelectronic packages.

Address correspondence to Professor Walter W. Yuen, Department of Mechanical Engineering, The Hong Kong Polytechnic University, Hung Hom, Kowloon, Hong Kong. E-mail: ppyuen@polyu.edu.hk

Color versions of one or more of the figures in the article can be found online at [www.tandfonline.com/uhte](http://www.tandfonline.com/uhte).

The objective of this work is to demonstrate the effectiveness of nonmetallic foam as a heat spreader, liquid wick, and heat sink material for an electronic package with localized high heat flux. In recent years, there has been a growing interest in using high-thermal-conductivity foam material for heat transfer applications [2–5]. For both single-phase [2] and multiphase flows [3–5], high-thermal-conductivity foams were demonstrated to be effective in providing heat transfer enhancement. For example, using graphite foam as an evaporator soldering directly to the back of silicon CMOS die in a thermosyphon [4], a cooling heat flux of 150 W/cm<sup>2</sup> was reported with the chip temperature maintained at less than 71°C. Since high-thermal-conductivity nonmetallic foams have many properties that are favorable for thermal management purposes (e.g., thermally stable, low in weight and density, chemically pure, low thermal expansion, resist thermal stress and shock, and inexpensive), additional studies to understand the heat transfer mechanisms and to determine the feasibility of using these materials for the cooling of optoelectronic packages with localized high heat flux are warranted.

Based on the geometry and heating requirement of a prototype package under consideration by an optoelectronic

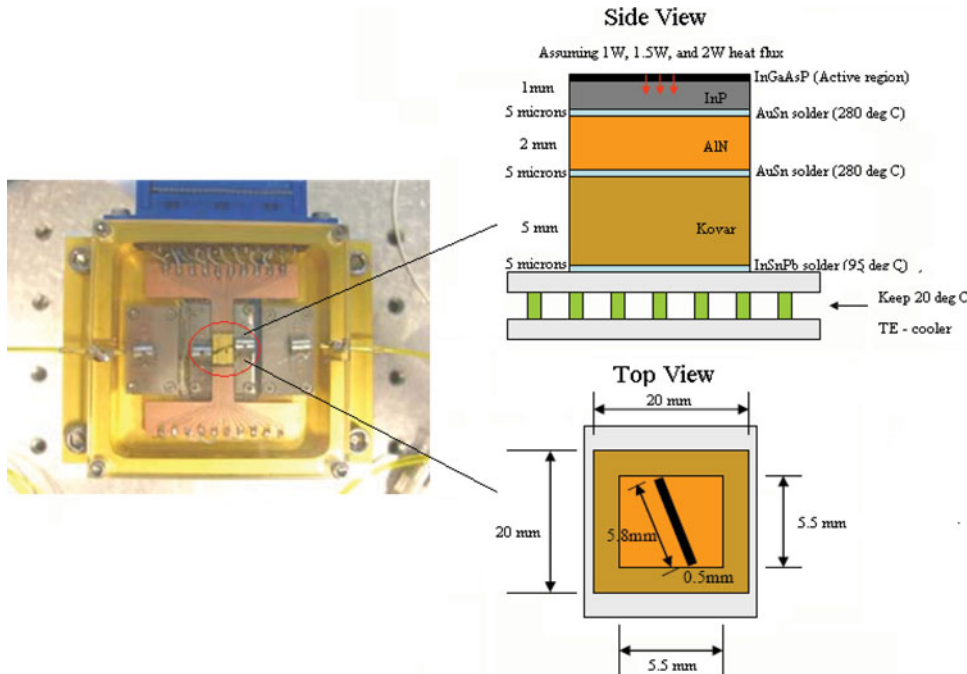


Figure 1 The prototype electronic package under consideration for cooling by the supercooler.

research group at the University of California at Santa Barbara, a graphite-foam-based “supercooler” is fabricated and its heat transfer performance is characterized experimentally. This paper summarizes result of the experimental and modeling efforts.

DESIGN OF THE “SUPERCOOLER”

The specific optoelectronic package used as a basis of the design of the supercooler is shown in Figure 1. As shown in the figure, the dimension of the heating area is small (5.8 mm by 0.5 mm). The active material (InGaAsP [indium gallium arsenite phosphate] and InP [indium phosphate]) is soldered to an aluminum nitrate (AlN) substrate that acts as a thermal spreader. The package is then soldered to Kovar, which is attached to a thermoelectric (TE) cooler for thermal control. The utilization of Kovar (which has a small coefficient of thermal expansion) is generally considered to be necessary to maintain the necessary optical alignment of the different components of the package.

The “supercooler” designed specifically to meet the thermal requirement of the package is shown in Figure 2. The heating area is simulated by depositing a thin resistive layer (with a dimension of 0.5 mm by 5 mm) on an AlN substrate. In contrast to the actual package, the AlN substrate is brazed to a Kovar slab only along its perimeter (approximately 1 mm width). The interior of the substrate is brazed to a graphite foam tip. The graphite foam tip is a part of a carbon foam cylindrical shell that is soaked with liquid water to allow for both high heat transfer and thermal diffusion within the solid carbon matrix and two-

phase boiling heat transfer in the porous region. The graphite foam shell is brazed to a copper cylindrical shell, which provides the outside mechanical support and heat-dissipating area for the supercooler. Cusil-ABA brazing alloy is used in the brazing process. The brazing temperature is 850°C.

An interior view of the supercooler and the relevant geometric dimensions are shown in Figure 3. The size of the copper cylinder is chosen so that there is sufficient area to dissipate the expected power input (1 to 10 W) by natural convection. The thickness of the graphite foam is selected largely based on practical constraints (the dimension of graphite foam available commercially and the brazing process).

The specific graphite foam used in the supercooler is POCO foam [6]. It has a thermal conductivity of 135 W/m-K in the out-of-plane direction and 45 W/m-K in the in-plane direction. Its

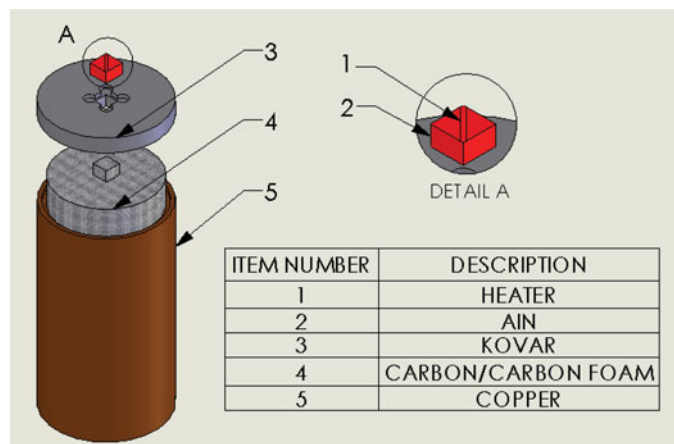
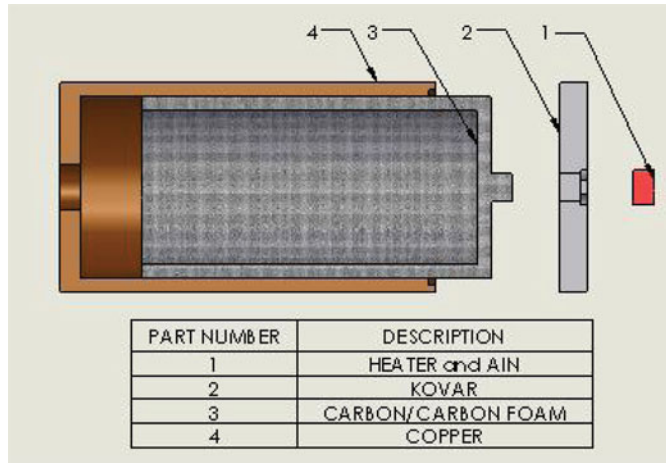


Figure 2 Schematic of the supercooler.



**Copper Cover Dimension**  
 $D = 3 \text{ cm}$ ,  $L = 5.4 \text{ cm}$

**Thickness of Carbon Foam Shell**  
 $d = 0.4 \text{ cm}$

**Figure 3** Interior view of the supercooler and the relevant geometric dimensions.

bulk density is 0.55 g/cc. The average pore diameter is 400  $\mu\text{m}$ , with an open porosity of 96% and a total porosity of 75%. The foam is selected because, in addition to its high thermal conductivity, the high porosity allows effective wicking flow for of the liquid coolant. A scanning electron micrograph (SEM) of the specific graphite foam used in the supercooler is shown in Figure 4.

Deionized water (18 M $\Omega$  DI water) is used as coolant. The DI water was degassed by boiling it for 20 minutes, repeated 3 times. Similar to heat pipe charging, the supercooler is sealed and evacuated down to  $10^{-6}$  torr prior to the experiment. A small amount of three-times deionized and degassed water (20 g) is then injected into the graphite foam shell to act as a two-phase coolant within the graphite foam. It should be noted that over

the period of 6 months when the experiment was conducted, there was no indication of degradation of the performance of the supercooler. The charging process for the coolant is thus effective.

## EXPERIMENTS

The experimental setup is shown in Figure 5a. A high-speed (1680-Hz) infrared camera (SBF-180) is the primary temperature measurement equipment used in the experiment. The camera is calibrated with a black-body source and the uncertainty in the temperature measurement is determined to be 0.5°C. To eliminate any uncertainty due to the effect of surface emissivity, the top of the supercooler, including the heating area, is coated with black paint. The experimental setup, with the heating surface of the supercooler facing upward, together with the camera, is shown in Figure 5b. Data were also obtained with the heating surface facing downward to assess the effect of gravity-driven buoyancy on the performance of the supercooler. All tests were conducted with no active cooling on the outside of the supercooler.

### Steady Heating

The maximum temperatures observed at the heating surface under a steady power input of 4 W and 10 W are shown in Figures 6a and 6b. At the initial stage of testing, there was a concern about securing good electrical contact to the thin resistive layer. Masking tape was wrapped around the mechanical contact on the side of the supercooler to ensure good electrical connection as shown in Figure 5a. This leads to additional thermal insulation and a slight increase in the maximum temperature as shown in Figure 6a. Subsequently, it was determined that good electrical contact was secured and all the remaining tests were conducted without the masking tape.

Data from the steady heating case show readily the high heat transfer capability of the supercooler. Based on the maximum

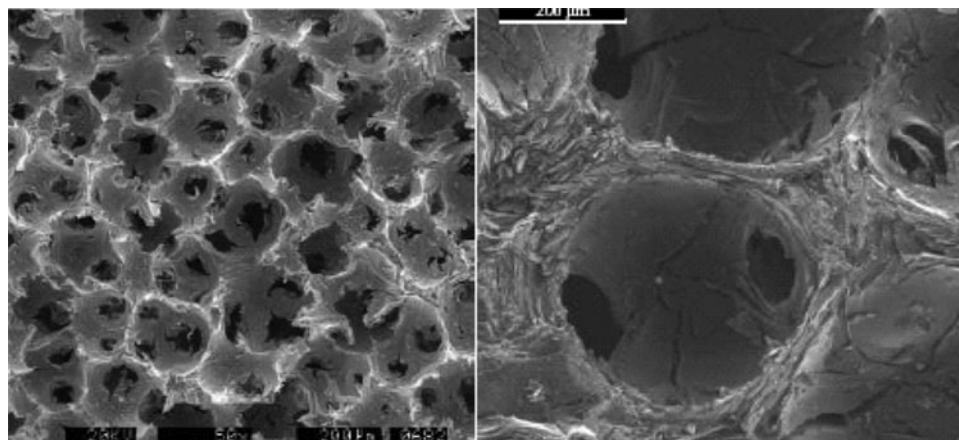


**Figure 4** SEM of the POCO Foam used in the supercooler.

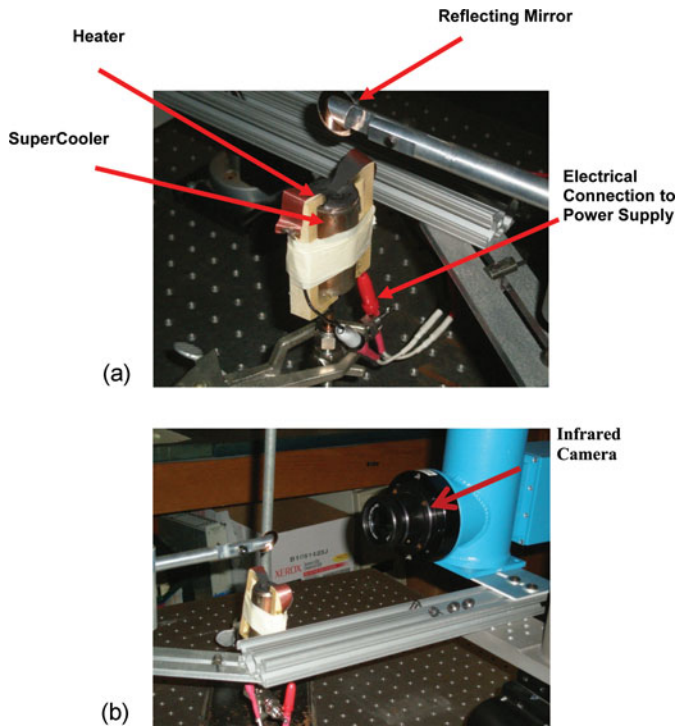


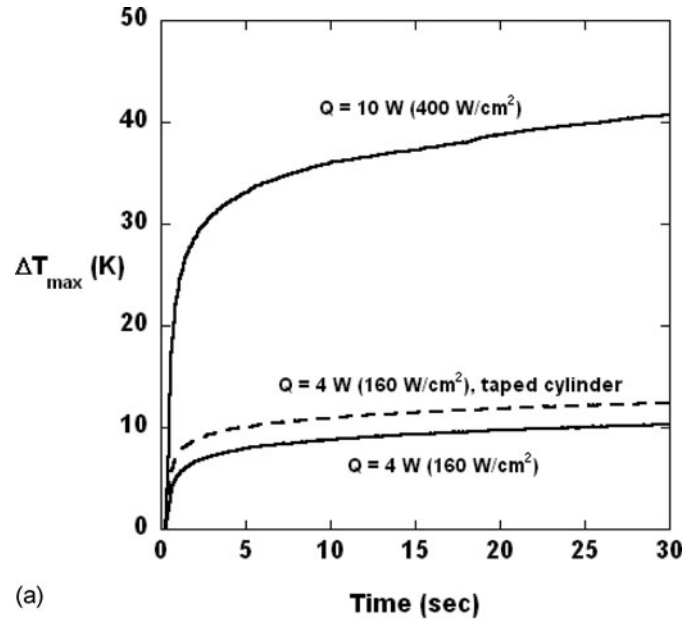
**Figure 5** (a) Top view of the experimental setup. (b) Experimental setup, together with the infrared camera used in the temperature measurement.

temperature observed and using the area of the heating element, the average heat transfer coefficients for the 4-W and 10-W case are approximately  $100 \text{ W}/(\text{m}^2\text{-K})$  and  $160 \text{ W}/(\text{m}^2\text{-K})$ , respectively. The effect of the heater orientation is shown in Figure 6b for the 10-W case. In general, the effect of the heater orientation appears to be insignificant. The slight variation in the maximum temperature can probably be attributed to experimental uncertainty (e.g., variation in setup, power input, ambient conditions, etc.). The lack of effect of the heater orientation demonstrates that the heat transfer in the supercooler is not driven by the gravity-driven buoyancy effect. Instead, the heat transfer is driven by the surface boiling at the heating surface and the wicking effect, which recirculates the liquid back to the heated surface.

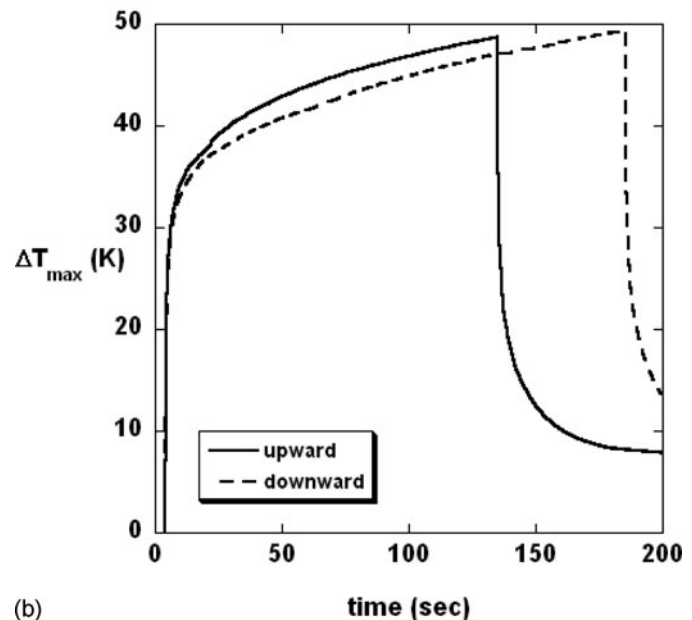
Even for the steady heating case, the supercooler showed a remarkable cooling capability, as the temperature of the surface drops rapidly (in less than 1 sec) after the power is turned off (see the 10-W case as shown in Figure 6b). This result demonstrates that the supercooler with carbon foam not only can lead to a high heat transfer coefficient, but is also a thermal diffuser that can diffuse heat quickly away from the high-temperature region when the heating is turned off.

### Periodic Heating

In view of the rapid temperature reduction and heat dissipation observed in the steady heating tests, a series of tests was



(a)



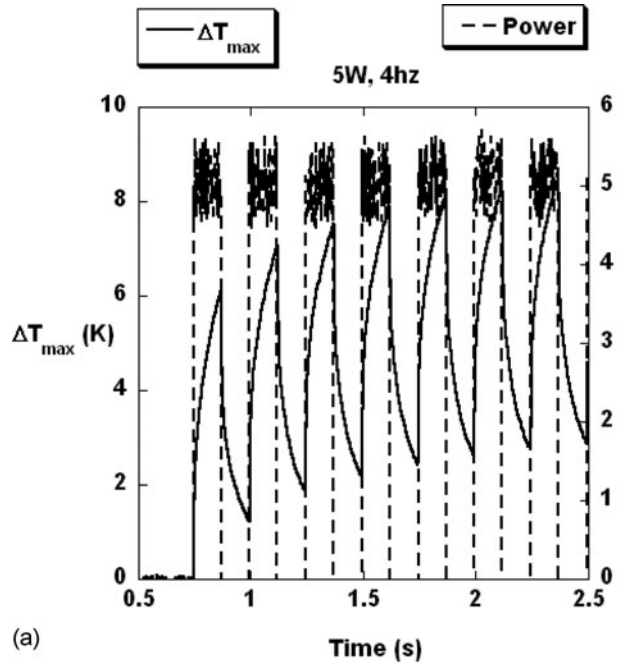
(b)

**Figure 6** (a) Effect of heating power for steady heating tests. (b) Effect of heater orientation for the steady heating test with 10 W.

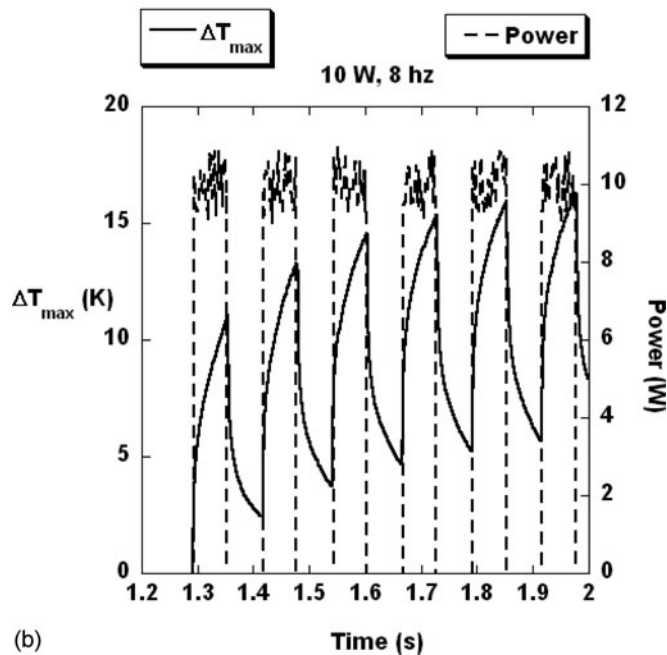
conducted to demonstrate the heat transfer behavior of the supercooler under the condition of a periodic heating input. Tests were conducted with a regular square-wave heating input (i.e., the power-on period equal to the power-off period) with a peak power of 5 W and 10 W with different frequencies (0.5 Hz, 1 Hz, 2 Hz, 4 Hz, and 8 Hz).

The maximum temperature rise for the 5-W-4-Hz and 10-W-8-Hz runs are shown together with the input power transient in Figures 7a and 7b. The two-dimensional (2D) infrared image of the top surface for the third and fourth heating cycle of the 10-W-8-Hz case and with the corresponding image for the





(a)



(b)

**Figure 7** (a) The input power transient, together with corresponding maximum temperature transient, for the 5-W-4-Hz run. (b) The input power transient, together with corresponding maximum temperature rise transient, for the 10-W-8-Hz run.

10-W steady heating case are shown in Figure 8. It can be readily observed that the supercooler showed a remarkable ability to dissipate heat, as the maximum temperature dropped almost instantaneously as the power is turned off. The rapid cooling effect is also felt uniformly across the whole top surface, away from the heating area, as shown by the two-dimensional infrared images shown in Figure 8.

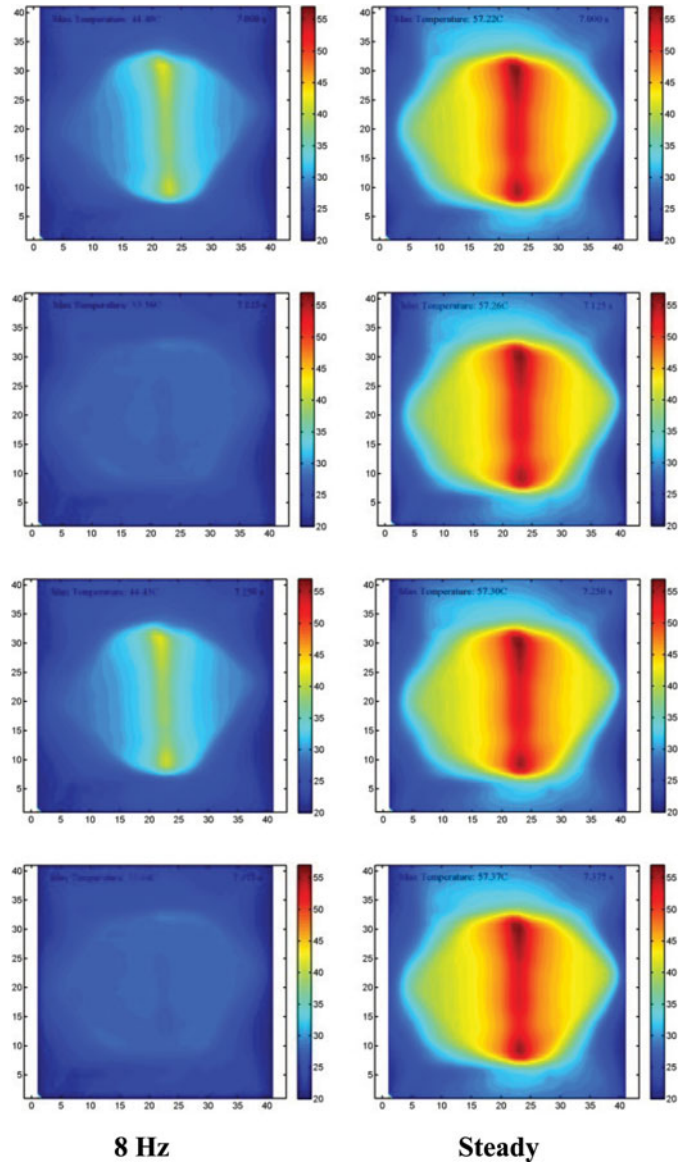


**Figure 8** The 2D infrared image of the heating surface for the third and fourth heating cycle of the 10-W-8-Hz run, together with the corresponding image for the 10W steady heating case. (The range of the temperature scale in these figures is 20°C to 55°C).

The maximum temperature rises for the 5-W and 10-W runs with different frequency, together with the corresponding steady heating run, are shown in Figures 9 and 10. For each of the periodic heating cases, the maximum temperature oscillates with the same frequency as the input power between an upper and lower bound, while the overall average temperature increases with time.

Plots of these upper and lower bounds at the different frequency for the two cases are shown in Figures 11a and 12a. Based on the reduction of the maximum temperature during the off period of the power input cycle, average cooling rates (K/s) for each cycle are estimated and shown in Figures 11b and 12b. It can be readily observed that the average cooling rate increases

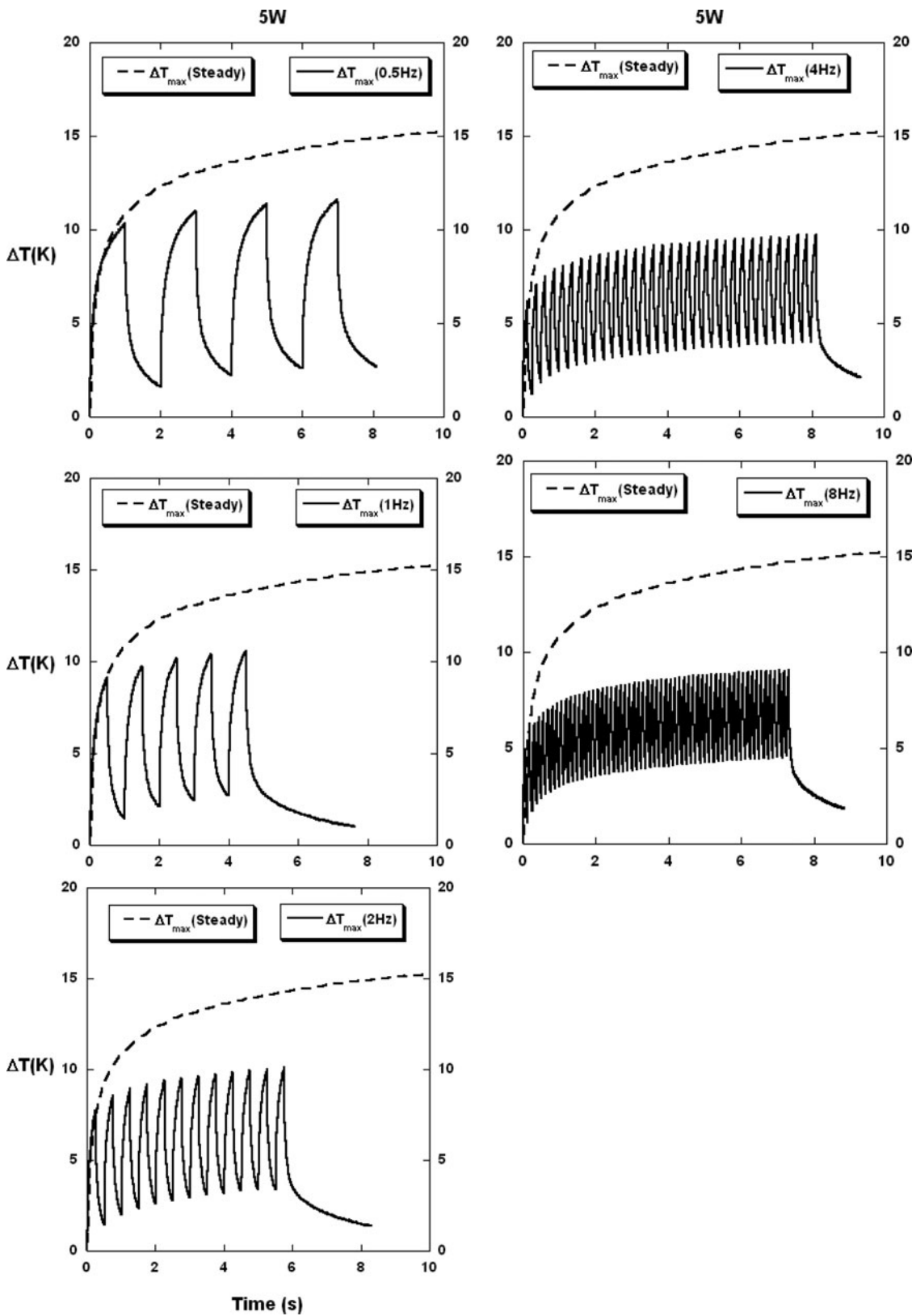


Figure 9 Maximum temperature rise for the 5-W periodic heating runs with different frequency, in comparison with the 5-W steady heating run.

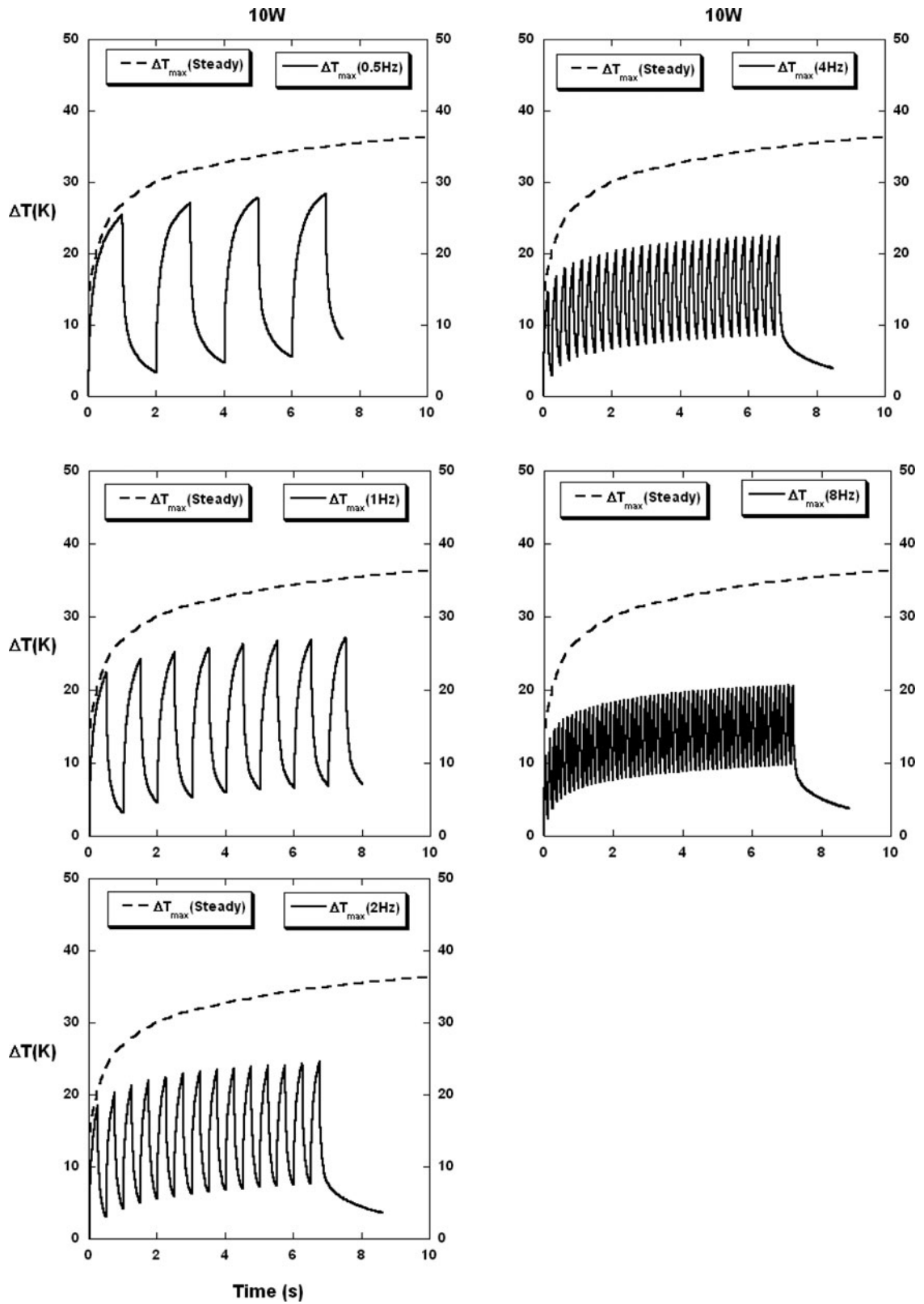
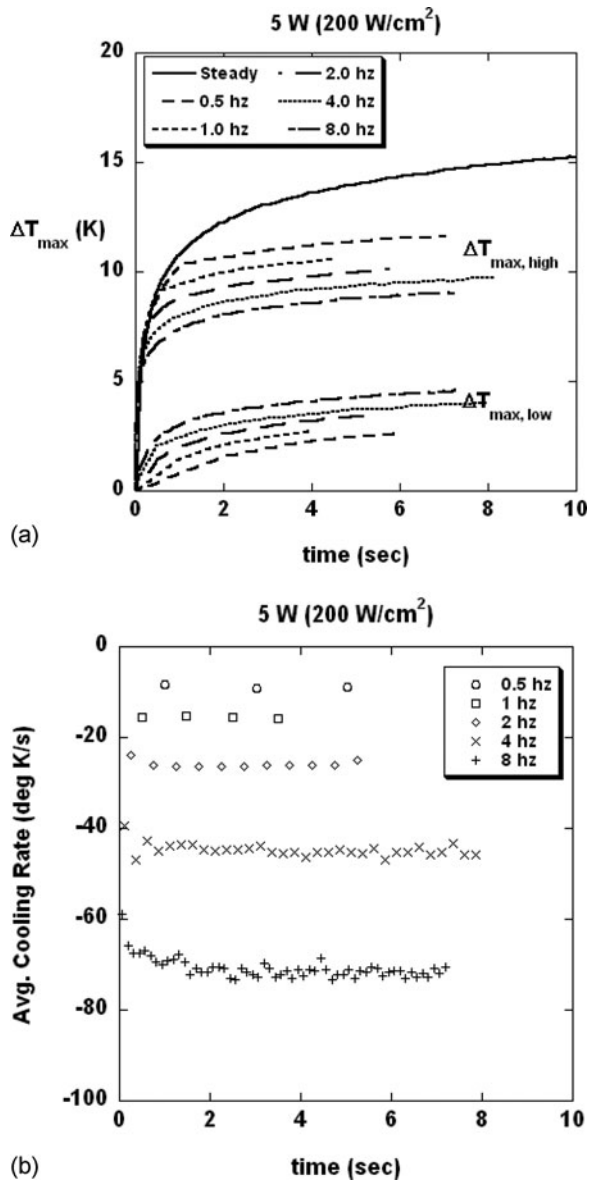


Figure 10 Maximum temperature rise for the 10-W periodic heating runs with different frequency, in comparison with the 5-W steady heating run.





**Figure 11** (a) The upper and lower bound of the maximum temperature rise for the 5-W periodic heating runs with different frequency, in comparison with the 5-W steady heating run. (b) The average cooling rate for the 5-W periodic heating runs with different frequency.

with increasing power and frequency, with a maximum rate of about 170 K/s. Physically, the heating characteristic of the supercooler under oscillatory heating is expected to approach the steady heating case in the limit of high frequency, when the characteristic time of cooling is much shorter than the period of oscillation. This result therefore suggests that the characteristic cooling rate of the supercooler is larger than 170 K/s, with a cooling time constant of less than 0.0625 sec (half of the period of an 8-Hz oscillation). Data in Figures 11a and 12a also show that as the frequency of the heating input increases, the maximum temperature oscillates with a narrower bound and a lower average temperature. The range of temperature is much lower than the corresponding maximum temperature rise for the steady

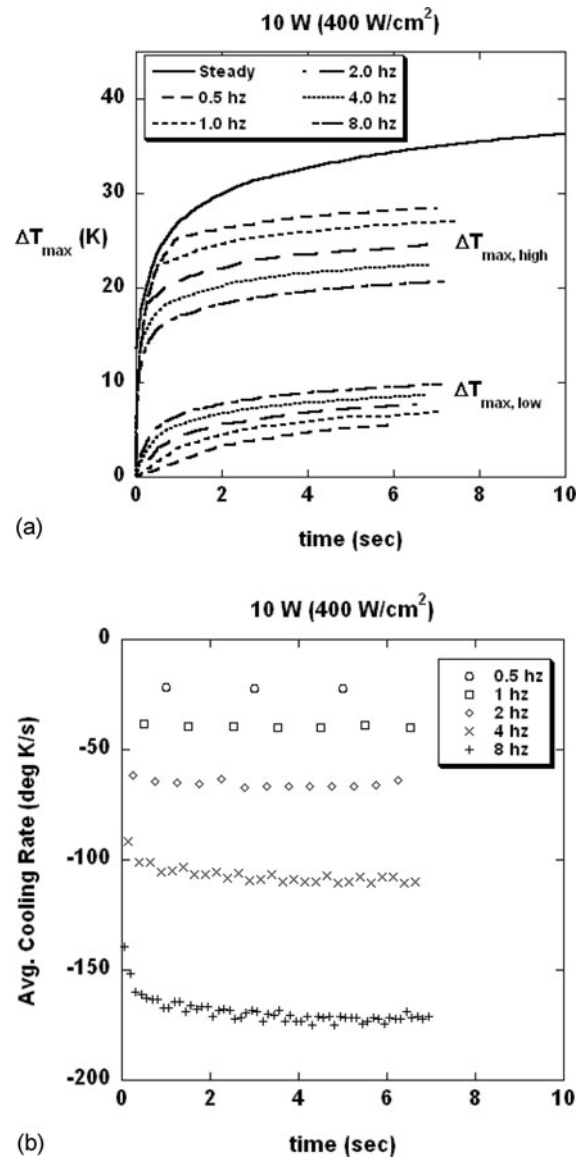


**Figure 12** (a) The upper and lower bound of the maximum temperature rise for the 10-W periodic heating runs with different frequency, in comparison with the 10-W steady heating run. (b) The average cooling rate for the 10-W periodic heating runs with different frequency.

heating case. For example, at 7 sec after the initial heating for the 10-W-8-Hz case, the upper and lower bound of the maximum temperature oscillation are at 20 K and 10 K above the ambient temperature respectively, while the maximum temperature for the 10-W steady heating case is at 35 K above ambient. Again, this lower average temperature can be attributed physically to the fact that the characteristic cooling time of the supercooler is less than 0.0625 sec. This result suggests that for thermal packages operating under a condition of highly localized periodic heating, the characteristic cooling time of the package should be included as one of the important design parameters in the assessment of a specific design.

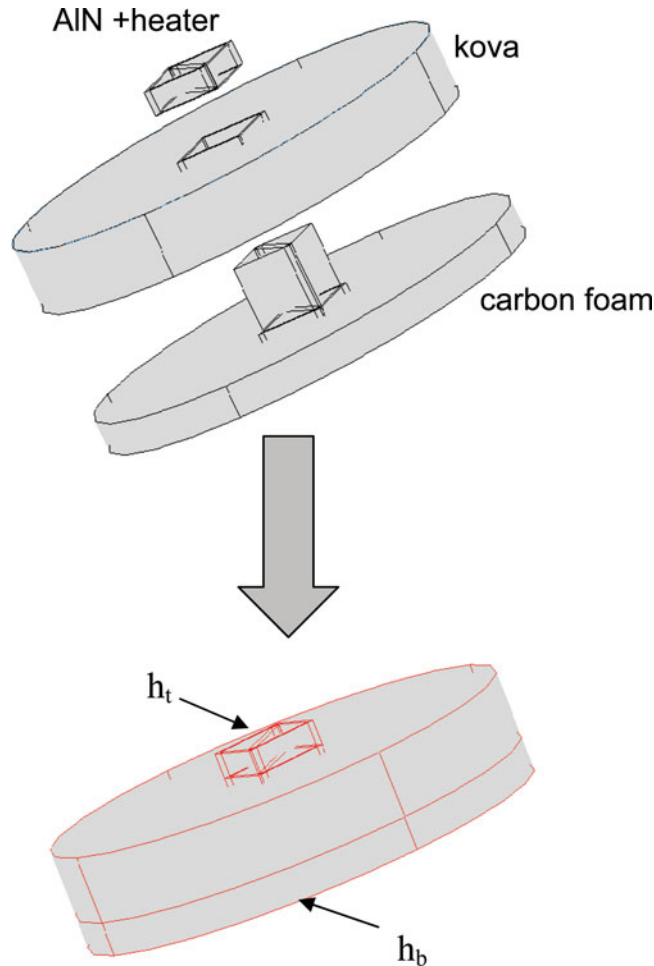


**Figure 13** Schematic of the supercooler geometry and the convective heat transfer boundary conditions modeled by COMSOL.

## ANALYSIS

A thermal model of the supercooler is constructed using COMSOL to understand the controlling physics of the heat transfer processes. A schematic of the model is shown in Figure 13. For simplicity and to focus the modeling effort on the initial heating period, the current model simulates only the top part of the supercooler accounting for the carbon foam, Kovar, and AIN structural design. “Contact resistance” is included in the model to account for the effect of joining (or brazing) different materials into one unit. The effect of the carbon foam and copper cylindrical shell will be important in the “long-time” thermal behavior of the supercooler. This effect will be considered in the future. The current model also does not include the presence of liquid water in the carbon foam. The mechanism of two-phase flow and boiling in carbon foam is currently not well understood. Convective heat transfer and boiling/condensation within the foam are thus not included in this model. An effective heat transfer coefficient at the bottom surface of the carbon foam

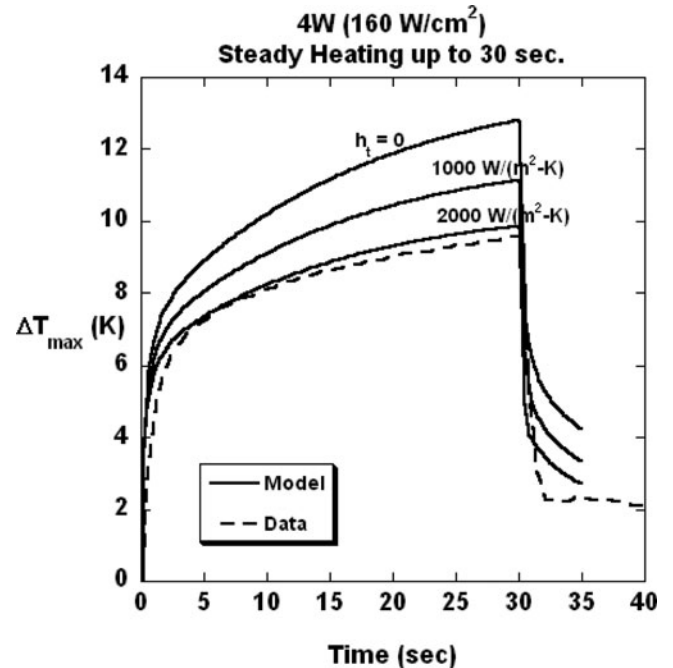


**Figure 14** Comparison between the COMSOL prediction of the maximum temperature increase and experiment for different values of the top heat transfer coefficient ( $h_t$ ) with a bottom heat transfer coefficient ( $h_b$ ) of  $1000 \text{ W/(m}^2\text{-K)}$ .

( $h_b$ ) and an effective heat transfer coefficient at the top surface of the AIN surface ( $h_t$ ) are used to account for the overall heat dissipation from the supercooler. Due to this simplification, the model is not expected to be able to simulate quantitatively all of the observed heat transfer behavior of the supercooler, particularly in cases with periodic heating. The model is thus intended only to provide some qualitative assessment of the heat transfer characteristics of the supercooler.

The 4-W steady heating case is the basis of the analytical study. Numerical experiments show that a relatively high heat transfer coefficient both at the surface of the AIN and at the bottom of the carbon foam base are needed to correlate the measured temperature rise. The predicted maximum temperature increase for different values of the top heat transfer coefficient  $h_t$  with a bottom heat transfer coefficient  $h_b = 1000 \text{ W/m}^2\text{-K}$  and different top heat transfer coefficient  $h_t$  are compared with the measured data and shown in Figure 14. A top heat transfer of  $h_t = 2000 \text{ W/m}^2\text{-K}$  appears to “fit” the measured maximum temperature increase effectively. When the power is turned off at 30 sec, the model also predicts accurately the rapid temperature reduction observed. The measured temperature distributions obtained by the infrared camera during the heating transient are compared with the COMSOL prediction in Figure 15. The model is quite effective in capturing the highly localized heating behavior around the heating region.

The relatively high values of the top and bottom heat transfer coefficient (e.g., the typical heat transfer coefficient in air is in the range of  $10\text{--}100 \text{ W/m}^2\text{-K}$ ) needed to correlate the experimental data show that the low pressure boiling within

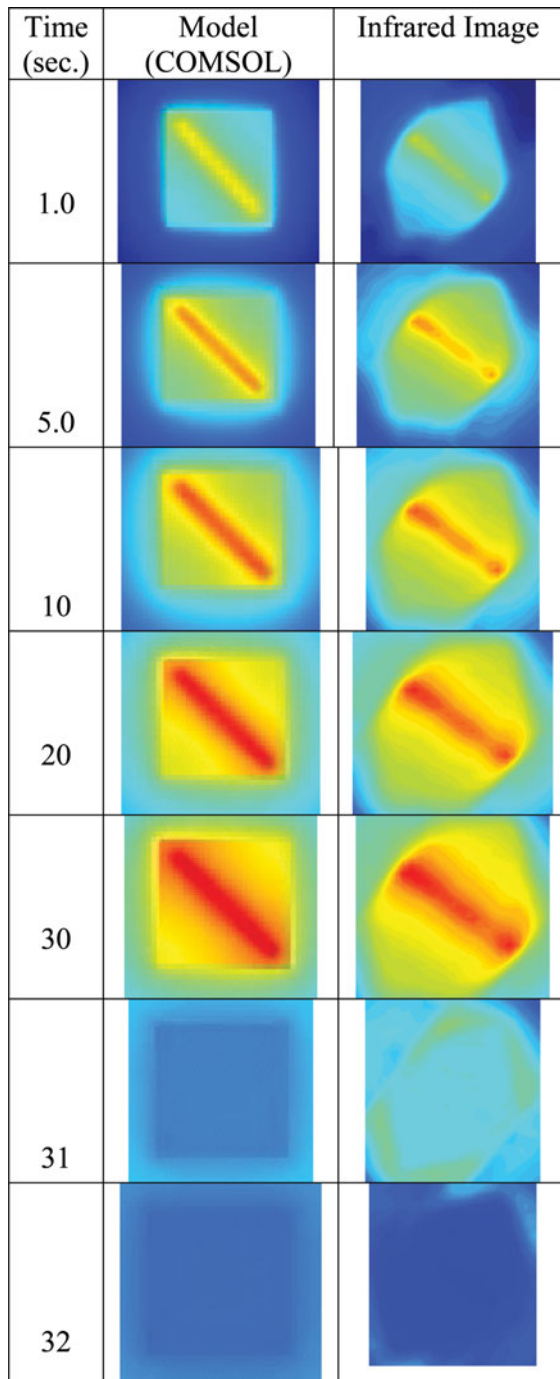


**Figure 15** Comparison between two-dimensional temperature distribution around the heater at different time as predicted by COMSOL (left) and measurement by the infrared camera (right). Note to the Editor: The corresponding author has agreed to pay the cost for color reproduction of Figure 15.

the supercooler has a definite role in the cooling process observed. This boiling mechanism and the wicking of liquid into the heated region need to be understood in the future design and improvement of the supercooler.

## CONCLUSIONS

A supercooler is fabricated using graphite foam as the primary heat transfer material for cooling. The graphite foam is soaked with water and the supercooler is operated under evacuated low pressure to ensure that two-phase boiling is occurring to enhance heat transfer. The specific design is directed toward the cooling of a prototypical optoelectronic package in which heat is generated in the order of 1 to 10 W over a region with dimension of 0.5 mm × 5 mm. The corresponding heat fluxes are 40 and 400 W/cm<sup>2</sup>.

Results show that carbon foam and the supercooler are effective in providing high heat transfer rate at the heating surface. Under a constant heating power input, the maximum temperature rise was maintained at a moderate level (40°C after 30 sec of heating with a power input of 10 W). The supercooler shows a remarkable capability to dissipate heat quickly and efficiently away from the heating area. Under periodic heating up to 8 Hz, the cooling rate was observed to exceed 170 K/s.

A numerical model of the supercooler, excluding the two-phase boiling/condensation effect, is developed using COMSOL. The model is effective in correlating the observed data. However, high heat transfer coefficients are required to obtain agreement with the measured data. An accurate understanding of the two-phase flow boiling/condensation process occurring within the carbon foam is clearly needed to further improve the performance of the supercooler and to adapt the technology to other high heat flux heating scenarios.

## FUNDING

This work is based on research supported under DARPA/MTO DoD-N and Army Program award number W911NF-04-9-0001. A slightly different version of this paper was also presented as paper IPACK2009-89008 at the 2009 ASME InterPACK Conference with a title of “Design and Testing of a Carbon Foam Based Supercooler for High Heat Flux Cooling in Optoelectronic Packages.”

## NOMENCLATURE

- d thickness (cm)
- D diameter (cm)
- $h_b$  top surface convective heat transfer coefficient (W/m<sup>2</sup>·K)
- $h_t$  bottom surface convective heat transfer coefficient (W/m<sup>2</sup>·K)
- L length (cm)
- Q input power (W)
- T temperature (K)

## REFERENCES

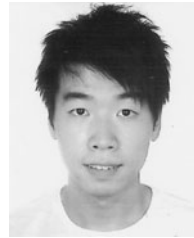
- [1] Blumenthal, D. J., Routing Packets With Light, *Scientific American*, pp. 82–85, 2001.
- [2] Gallego, N. C., and Klett, J. W., Carbon Foams for Thermal Management, *Carbon*, vol. 41, pp. 1461–1466, 2003.
- [3] Lin, S., Sefiane, K., and Christy, J. R. E., Prospect of Confined Flow Boiling in Thermal Management of Microsystems, *Applied Thermal Engineering*, vol. 22, pp. 825–837, 2002.
- [4] Klett, J. W., and Trammel, M., Parametric Investigation of a Graphite Foam Evaporator in a Thermosyphon with Fluorinert and a Silicon CMOS Chip, *IEEE Transactions on Device and Materials Reliability*, vol. 4, no. 3, pp. 626–637, 2004.
- [5] Topin, F., Bonnet, J.-P., Madani, B., and Tardist, L., Experimental Analysis of Multiphase Flow in Metallic foam: Flow Laws, Heat Transfer and Convective Boiling, *Advanced Engineering Materials*, vol. 8, no. 9, pp. 890–899, 2006.
- [6] Poco Graphite, Inc., Decatur, TX.



**Walter W. Yuen** is the Vice President (Academic Development) as well as a Chair Professor at the Department of Mechanical Engineering and Building Service Engineering Department at the Hong Kong Polytechnic University. His research is in the areas of thermal radiation heat transfer, two-phase flow, and electronic cooling. He was a professor of mechanical engineering at the University California at Santa Barbara (UCSB) until 2009. Much of the research reported in this paper was done while he was at UCSB.



**Jianping Tu** is currently a research engineer at All-comp, Inc., a carbon-based materials R&D company at the City of Industry, California. He was previously a research associate at the University of California at Santa Barbara, where much of the work of this paper was conducted. His research expertise is in the areas of heat exchangers and heat transfer enhancement.



**Wai-Cheong Tam** is currently a Ph.D. student in mechanical engineering at the Hong Kong Polytechnic University. He received an M.S. degree from the University of California.



**Daniel J. Blumenthal** is a professor in the Department of Electrical and Computer Engineering at the University of California, Santa Barbara. He is Director of the Terabit Optical Ethernet Center (TOEC). He serves on the Internet2 Architecture Advisory Council. His research interests are in optical communications, photonic packet switching and all-optical networks, all-optical wavelength conversion and regeneration, ultrafast communications, InP Photonic Integrated Circuits (PICS), and nanophotonic device technologies. He is recipient of a Presidential Early Career Award for Scientists and Engineers from the White House, a National Science Foundation Young Investigator Award, and an Office of Naval Research Young Investigator Program Award.